Journal of Fluorine Chemistry 220 (2019) 41–47

Contents lists available at ScienceDirect

Journal of Fluorine Chemistry

journal homepage: www.elsevier.com/locate/fluor

# A metastable $[(MgF_3)_2]^{2-}$ dianion composed of two superhalogen anions

Sylwia Freza[a,*], Iwona Anusiewicz[a], Jack Simons[b], Piotr Skurski[a,b]

[a] Laboratory of Quantum Chemistry, Faculty of Chemistry, University of Gdańsk, Wita Stwosza 63, 80-308, Gdańsk, Poland
[b] Henry Eyring Center for Theoretical Chemistry, Department of Chemistry, University of Utah, Salt Lake City, UT, 84112, United States

ARTICLE INFO

*Keywords:*
Dianion
Repulsive Coulomb Barrier
Superhalogen

ABSTRACT

The electronic and thermodynamic stabilities of the $[(MgF_3)_2]^{2-}$ dianion (composed of two neutral radical superhalogen $MgF_3$ molecules and two excess electrons) are investigated on the basis of theoretical calculations employing ab initio methods. It is demonstrated that this species is vertically and adiabatically electronically stable (by 5.58 and 2.28 eV, respectively). Although it is susceptible to certain fragmentations, $[(MgF_3)_2]^{2-}$ is predicted to be kinetically long-lived (due to substantial energy barriers for any of the fragmentation reactions) and thus it is likely to be detected in electrospray mass spectroscopic studies if solutions containing salts of this dianion can be formed. For this reason, the structures and energies of the corresponding $Na_2[(MgF_3)_2]$ salt are also examined as part of this study.

## 1. Introduction

Superhalogens are commonly defined as compounds exhibiting high electron affinities (3.6–14 eV) [1–3] exceeding those of halogen atoms. The existence of such species was predicted in 1981 by Gutsev and Boldyrev who employed quantum chemistry methods to support their hypothesis [1]. In addition, they proposed a simple formula for one class of superhalogens, $MX_{k+1}$ and the corresponding superhalogen anions $[MX_{k+1}]^-$, where M is a main group or transition metal atom, X is a halogen atom, and k is the maximal formal valence of the atom M. Since the 1980's many scientific reports describing various superhalogens have been published [4–19] including a milestone work comprising the first experimental photoelectron spectra of superhalogen anions (measured by the Wang group) together with their theoretical interpretations provided by Boldyrev and Simons [20]. During last two decades it was also revealed that superhalogens might alternatively be composed of non-metal central atoms [21,22] or nonhalogen ligands [23–29]. In addition, the existence and stability of so-called 'hyperhalogens' (i.e., compounds with the $MX_{k+1}$ formula but containing superhalogens themselves as ligands X) has been confirmed [30–33].

Despite their very large first electron affinities, superhalogens (either mononuclear $MX_{k+1}$ or polynuclear $M_nX_{nk+1}$ (where n stands for the number of central atoms)) seem to not be capable of binding two excess electrons. This likely is due to the fact that a typical $MX_{k+1}$ (or $M_nX_{nk+1}$) superhalogen molecule is an open-shell system having one unpaired electron thus the attachment of one excess electron results in a closed-shell structure with no half-filled or empty molecular orbital to hold a second excess electron.

Therefore, a main goal of this work was to consider the possibility of forming stable or metastable dianions composed of two $MX_{k+1}$ superhalogen building blocks with two excess electrons. Even though the Coulomb repulsion in such a $[(MX_{k+1})_2]^{2-}$ could be anticipated to be very large, the strong ability to bind an excess electron exhibited by each of its binding sites could still render the $[(MX_{k+1})_2]^{2-}$ dianion stable to autodetachment of an electron or to Coulomb explosion.

In this contribution we present the results of theoretical studies concerning the $[(MgF_3)_2]^{2-}$ dianion. We describe the equilibrium structure of this unusual system and discuss its stability with respect to fragmentation and to autodetachment of an excess electron. In addition, we investigate the role that the Repulsive Coulomb Barrier (RCB) [34–37] plays for the predicted electronic stability of such a doubly negatively charged superhalogen dimer. We also examine the stability and structure of a possible $Na_2[(MgF_3)_2]$ salt containing two $Na^+$ cations and the $[(MgF_3)_2]^{2-}$ dianion.

## 2. Methods

The equilibrium structures of the systems investigated in this work were obtained by applying the second-order Møller-Plesset (MP2) perturbation method [38–40] with the 6311 + G(d) basis set [41,42]. The harmonic vibrational frequencies characterizing the stationary points were evaluated at the same MP2/6-311 + G(d) level to assure that all the obtained structures correspond to true minima or first order saddle

---

* Corresponding author at: Faculty of Chemistry, University of Gdańsk, Wita Stwosza 63, 80-308 Gdańsk, Poland.
*E-mail address:* sylwia.freza@ug.edu.pl (S. Freza).

https://doi.org/10.1016/j.jfluchem.2019.02.007
Received 7 January 2019; Received in revised form 18 February 2019; Accepted 18 February 2019

points on the potential energy surface. The coupled-cluster method with single, double, and non-iterative triple excitations (CCSD(T)) [43–46] was then employed to refine the electronic energies of all stationary point structures (using the same 6-311 + G(d) basis set). The intrinsic reaction coordinate (IRC) procedure [47–50] (during which the reaction path is followed in both directions away from the transition state) was employed to confirm the corresponding minima for each transition structure.

The first vertical electron detachment energy (VDE) of the $[(MgF_3)_2]^{2-}$ dianion structure was obtained by employing the outer valence Green function OVGF method (*B* approximation) [51–59], which is closely related to so called ‘equations of motion (EOM)’ approaches. Since the OVGF approximation remains valid only for outer valence ionizations for which the pole strengths (PS) are greater than 0.80-0.85 [60], we verified that the PS value was sufficiently large to justify the use of the OVGF method for each of the states studied here (the PS found for the state examined in this work was 0.945). We used the larger 6-311 + G(3df) basis while estimating the first vertical electron binding energy of $[(MgF_3)_2]^{2-}$ since analogous basis sets have been used for superhalogen anions and provided an excellent agreement between such calculated and experimentally measured VDEs [6,16,18,20,61].

The partial atomic charges were evaluated by the Natural Bond Orbital (NBO) analysis scheme [62–66]. All calculations were performed using the GAUSSIAN16 (Rev. B.01) package [67].

## 3. Results and discussion

The equilibrium $D_{2h}$-symmetry structure of the $[(MgF_3)_2]^{2-}$ dianion can be viewed as consisting of two quasi-tetrahedral $MgF_4$ fragments sharing two fluorine atoms as shown in Fig. 1. The bond lengths between Mg atoms and terminal F atoms are shorter by 0.096 Å than those in the Mg-F-Mg bridging fragments. It is important to stress that this structure of $[(MgF_3)_2]^{2-}$ is geometrically stable (i.e., it corresponds to a minimum on the dianion’s potential energy surface). In addition, $[(MgF_3)_2]^{2-}$ is vertically electronically stable as its first vertical electron detachment energy was calculated to be 5.58 eV. As far as the adiabatic electronic stability of $[(MgF_3)_2]^{2-}$ is concerned, we confirmed that the energy of this dianion is lower by 2.28 eV (52.6 kcal/mol) than the energy of the most stable isomer of $[(MgF_3)_2]-$ depicted in Fig. 2 (see $[(MgF_3)_2]^-$ (**1**)).

Photo-ejecting one excess electron from $[(MgF_3)_2]^{2-}$ would initially populate a different (local minimum) isomeric structure of the $[(MgF_3)_2]^-$ monoanion (shown in Fig. 2 as $[(MgF_3)_2]^-$ (**2**)) whose structure mimics the equilibrium structure of $[(MgF_3)_2]^{2-}$. Since the isomer $[(MgF_3)_2]^-$ (**2**) is higher in energy by 1.95 eV (44.9 kcal/mol) than $[(MgF_3)_2]^-$ (**1**) (and by 4.23 eV (97.5 kcal/mol) than the $[(MgF_3)_2]^{2-}$ dianion), one can expect (**2**)→(**1**) isomerization to follow, but at a rate depending on the barrier of 13.1 kcal/mol connecting these two structures (the height of the barrier was calculated at the CCSD(T)/6-311 + G(d) level, see also Fig. 2 for the corresponding TS(**2**)→(**1**) structure).

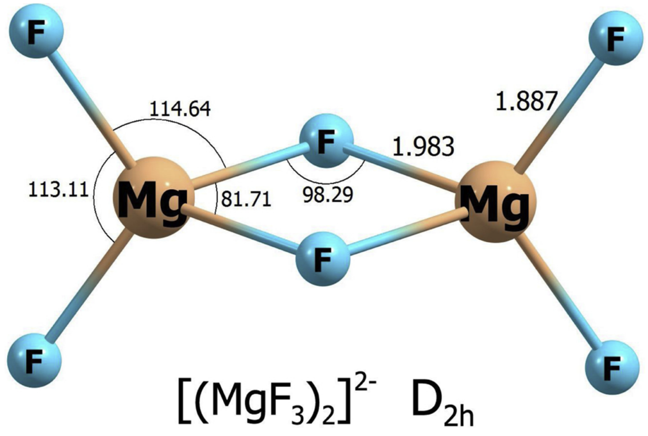

**Fig. 1.** Equilibrium structure of $[(MgF_3)_2]^{2-}$. Bond lengths in Å, valence angles in degrees.

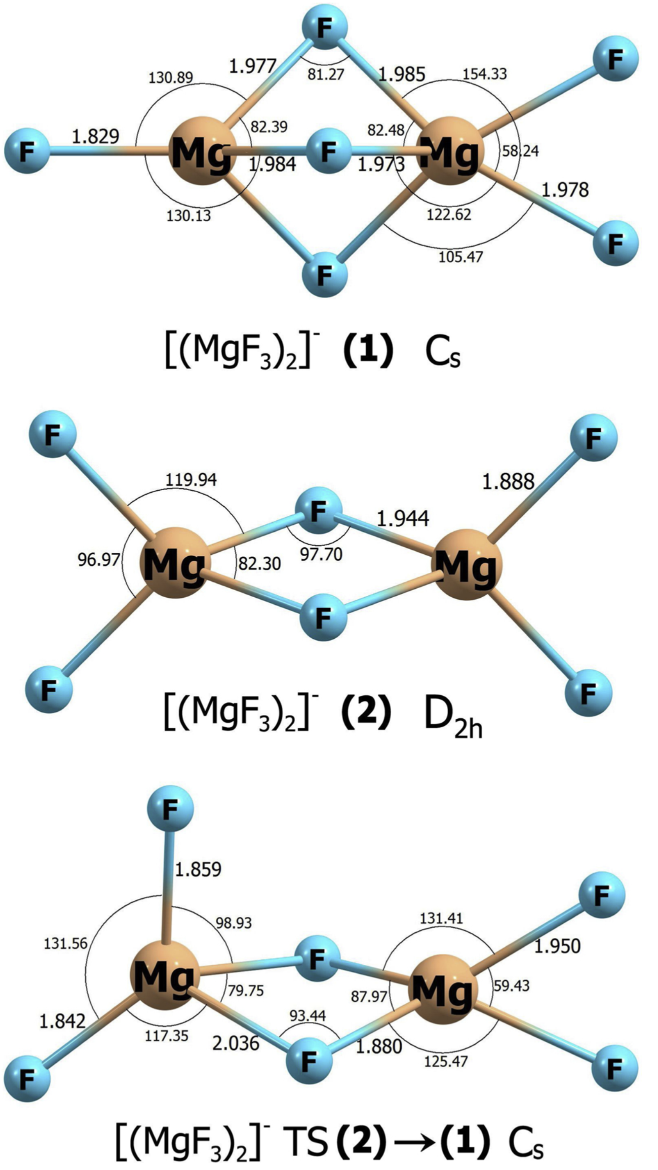

**Fig. 2.** Equilibrium structures of $[(MgF_3)_2]^-$ monoanions: the lowest energy isomer of $[(MgF_3)_2]^-$ ((**1**), top), the second isomer of $[(MgF_3)_2]^-$ ((**2**), center), and the transition state structure connecting these minima (TS(**2**)→(**1**), bottom). Bond lengths in Å, valence angles in degrees.

In order to examine the thermodynamic stability of $[(MgF_3)_2]^{2-}$ we considered seven different fragmentation paths including: (i) the loss of $F^-$ and formation of either $[Mg_2F_5]^-$ or of $[MgF_3]^-$ and $MgF_2$ ; (ii) the loss of $[F_2]^-$ and formation of either $[Mg_2F_4]^-$ or of $[MgF_3]^-$ and MgF ; (iii) the fragmentation to $[MgF_3]^-$, $[MgF]^-$, and $F_2$; (iv) the loss of two $F^-$ anions and formation of $Mg_2F_4$; and (v) fragmentation into two $[MgF_3]^-$ anions (see Table 1). As indicated by the calculated energies for these reactions ($\Delta E_r$), $[(MgF_3)_2]^{2-}$ is predicted to be susceptible only to fragmentations leading to either $[Mg_2F_5]^-$ and $F^-$ or to two $[MgF_3]^-$ anions. In particular, the most probable fragmentation path (i.e., leading to the most stable final products) corresponds to the formation of two very stable superhalogen $[MgF_3]^-$ anions whose combined energy is lower by 13.9 kcal/mol than that of $[(MgF_3)_2]^{2-}$.

**Table 1**
The reaction energies[a] ($\Delta E_r$ in kcal/mol) evaluated for various fragmentation processes involving the $[(MgF_3)_2]^{2-}$ dianion.

| Process | $\Delta E_r$ |
|---|---|
| $[(MgF_3)_2]^{2-} \rightarrow 2[MgF_3]^-$ | −13.9 |
| $[(MgF_3)_2]^{2-} \rightarrow [Mg_2F_5]^- + F^-$ | −3.7 |
| $[(MgF_3)_2]^{2-} \rightarrow [MgF_3]^- + MgF_2 + F^-$ | 79.9 |
| $[(MgF_3)_2]^{2-} \rightarrow [MgF_3]^- + [MgF]^- + F_2$ | 222.0 |
| $[(MgF_3)_2]^{2-} \rightarrow [MgF_3]^- + MgF + [F_2]^-$ | 184.7 |
| $[(MgF_3)_2]^{2-} \rightarrow Mg_2F_4 + 2F^-$ | 108.7 |
| $[(MgF_3)_2]^{2-} \rightarrow [Mg_2F_4]^- + [F_2]^-$ | 134.0 |

[a] Reported $\Delta E_r$ values include zero-point vibrational energies.

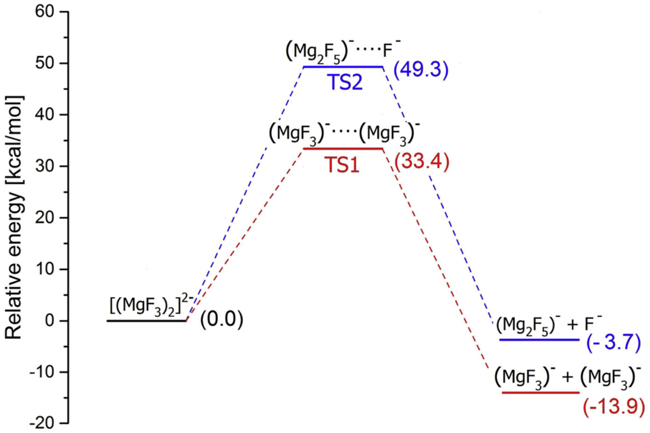

**Fig. 3.** Schematic energy profiles for two fragmentation paths of $[(MgF_3)_2]^{2-}$. Relative energies (in kcal/mol) of the stationary points are given in parentheses.

Since we found two possible paths along which the fragmentation of $[(MgF_3)_2]^{2-}$ is energetically favorable (see Table 1), we decided to take a closer look at these processes. For each of these fragmentations (i.e., $[(MgF_3)_2]^{2-} \rightarrow 2[MgF_3]^-$ and $[(MgF_3)_2]^{2-} \rightarrow [Mg_2F_5]^- + F^-$), we searched for kinetic barriers separating $[(MgF_3)_2]^{2-}$ and the products. We found the transition state (TS) structures corresponding to both fragmentation paths and we performed intrinsic reaction coordinate calculations during which the reaction paths were followed in both directions (by integrating the intrinsic reaction coordinate). According to these IRC calculations, we confirmed that each of the transition structures indeed connects the expected minima on the reaction paths presented in Fig. 3.

The structures of the TS1 and TS2 transition states (corresponding to $[(MgF_3)_2]^{2-} \rightarrow 2[MgF_3]^-$ and $[(MgF_3)_2]^{2-} \rightarrow [Mg_2F_5]^- + F^-$, respectively) are depicted in Fig. 4. The separation between the two $MgF_3$ fragments (which correspond to the fragmentation products) is relatively large in TS1 (3.486 Å) while both of these units adopt a quasi-triangular structure (approaching the planar triangular $D_{3h}$-symmetry structure exhibited by the isolated $[MgF_3]^-$ monoanion (see Fig. 4 and Ref. [68]). The results of the NBO population analysis performed for TS1 confirms that these two $MgF_3$ fragments may be treated as $[MgF_3]^-$ monoanions because their partial atomic charges sum up to -1.001*e* and -0.999*e*. On the other hand, the $C_s$-symmetry structure of TS2 resembles that of the $[Mg_2F_5]^-$ product (shown in Fig. 4) with a distant $F^-$ anion (separated by 3.894 Å from the Mg atom). Again, the population analysis confirms that each of these two fragments holds ca. -1*e* excess charge as the partial atomic charge on F is equal to -0.998*e* while the partial atomic charges on the remaining fragment sum up to -1.002*e*.

As mentioned in the preceding paragraphs, there are two energetically favorable fragmentation paths for $[(MgF_3)_2]^{2-}$ (see Table 1), namely, $[(MgF_3)_2]^{2-} \rightarrow 2[MgF_3]^-$ and $[(MgF_3)_2]^{2-} \rightarrow [Mg_2F_5]^- + F^-$. However, the energies of the transition states found for these processes indicate that the kinetic barriers that have to be overcome to complete these fragmentations are relatively large and equal to 33.4 and 49.3 kcal/mol, respectively. Therefore, the expected rate of passage over any of these two barriers renders the $[(MgF_3)_2]^{2-}$ dianion kinetically very long-lived except at very high temperatures or with some other source of high internal energy.

Having discussed the stability of $[(MgF_3)_2]^{2-}$ regarding possible structural reorganization, we move on to the analysis of the excess electron binding energies. As already mentioned in the preceding paragraphs, $[(MgF_3)_2]^{2-}$ is vertically electronically stable by 5.58 eV. Albeit relatively large, this stability is significantly smaller than that of the $[MgF_3]^-$ monoanion (8.79 eV [68]). $[(MgF_3)_2]^{2-}$ is in fact composed of two $[MgF_3]^-$ monoanions, hence one might expect each of its two $MgF_3$ sites to bind an excess electron by 8.79 eV. Clearly, this would be the case only for two singly negatively charged $[MgF_3]^-$ fragments separated by infinitely large distance (i.e., not interacting with each other). However, when the distance between two $[MgF_3]^-$ systems becomes finite, the Coulomb repulsion between the two anionic sites decreases the electron binding abilities of both sites.

The positive value electron binding energy determined for $[(MgF_3)_2]^{2-}$ indicates that the Coulomb repulsion potential is not strong enough to outweigh the valence-region attractive potentials of each $MgF_3$ site. As a consequence, the doubly charged anion $[(MgF_3)_2]^{2-}$ is electronically stable with respect to the singly charged $[(MgF_3)_2]^-$ anion. Although $[(MgF_3)_2]^{2-}$ is composed of two $MgF_3$ fragments (each of which is capable of binding an excess electron by 8.79 eV), the dianion's first electron binding energy is only 5.58 eV because to remove an electron from one of the two $MgF_3$ fragments assembled into the $[(MgF_3)_2]^{2-}$ dimer does not require as much energy as for the singly charged $[MgF_3]^-$ due to the Coulomb repulsion energy generated by the other negative charge localized on the neighboring $MgF_3$ moiety. Although the influence of this destabilizing effect is rather easy to estimate for large finite separations between $MgF_3$ sites, the situation is more complicated when two such fragments are assembled into one molecular system, as it is the case for the $[(MgF_3)_2]^{2-}$ dianion. However, we can utilize the *extended Repulsive Coulomb Barrier model* to treat structurally compact multiply charged anions and described in Ref. [34].

According to the *extended RCB model*, the Coulomb repulsion between two excess electrons can be thought of as raising the energy level of the bound electron by an amount $e^2/R$ that depends on the distance $R$ between the electron being detached and the other negatively charged site. While using this model it is important to note that the vertical dianion-monoanion energy difference has to be calculated at the equilibrium structure of the dianion because the Coulomb model relates to energy differences among species having the same atomic composition and nuclear positions but varying number of electrons, and thus should be viewed as a means for predicting vertical rather than adiabatic electron detachment energies [34]. The internal Coulomb energy for $[(MgF_3)_2]^{2-}$ can be evaluated by computing $e^2/R_{LL}$ for each resonance structure of this species and averaging over the resonance structures (where $R_{LL}$ stands for the ligand-ligand separation, i.e., the separation between the atoms where the excess charges are assumed to be localized). Even though $[(MgF_3)_2]^{2-}$ contains 6 electronegative fluorine atoms where the excess electrons could potentially be localized, analysis of the ab initio electron density distribution in this system allows us to limit that number to 4 by excluding the two F atoms localized in the central fragment and involved in the Mg-F-Mg bonds. Indeed, the highest occupied molecular orbital (HOMO) in $[(MgF_3)_2]^{2-}$ holding two excess electrons is delocalized exclusively among the four terminal

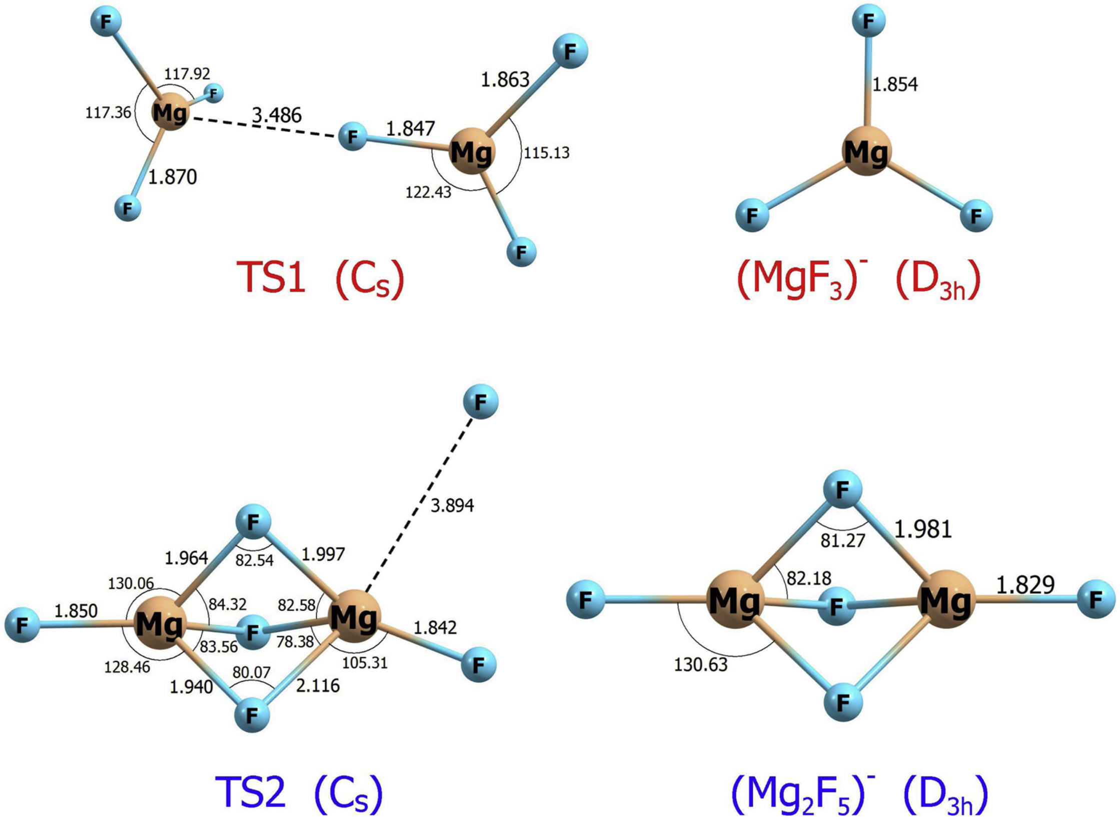

**Fig. 4.** The structures of the transition states (TS) and products of the $[(MgF_3)_2]^{2-} \rightarrow 2[MgF_3]^-$ (TS1) and $[(MgF_3)_2]^{2-} \rightarrow [Mg_2F_5]^- + F^-$ (TS2) fragmentation reactions. Bond lengths in Å, valence angles in degrees.

fluorine atoms (see Fig. 5) because locating excess electron density on either of the bridging F atoms would generate higher repulsive internal Coulomb energy and thus raise the total energy of the species.

Hence, while applying the *extended RCB model* to estimate the internal Coulomb energy for $[(MgF_3)_2]^{2-}$, it is sufficient to consider only 3 resonance structures in which the two excess charges are assumed to be separated by either $R_1$, $R_2$, or $R_3$, as defined in Fig. 5. Since the four terminal F atoms in $[(MgF_3)_2]^{2-}$ are equivalent due to symmetry, one can view one of the excess charges as residing on any one of these sites with the second negative charge residing $R_1$, $R_2$, or $R_3$ away. Assuming that these three distances occur with equal weight, we can estimate the internal Coulomb energy in the $[(MgF_3)_2]^{2-}$ dianion minus that of the $[(MgF_3)_2]^-$ monoanion (which is zero) as:

$$\textit{Internal Coulomb Energy} = \frac{1}{3}\left(\frac{e^2}{R_1} + \frac{e^2}{R_2} + \frac{e^2}{R_3}\right)$$

Introducing $R_1 = 5.081$ Å, $R_2 = 5.978$ Å, and $R_3 = 3.150$ Å (i.e., the separations corresponding to the equilibrium structure of $[(MgF_3)_2]^{2-}$ and defined in Fig. 5) into this equation results in an internal Coulomb energy of 3.27 eV. The value of 3.27 eV is very close to 3.21 eV (i.e., the difference between the excess electron binding energy of the $[MgF_3]^-$ monoanion (8.79 eV) and the ab initio first excess electron binding energy of the $[(MgF_3)_2]^{2-}$ dianion (5.58 eV)), which confirms the usefulness and applicability of the *extended RCB model*. Summing up, one may consider each of the $MgF_3$ electron binding sites in $[(MgF_3)_2]^{2-}$ as being destabilized by ca. 3.2–3.3 eV due to the presence of the second $MgF_3$ electron binding site.

Finally, we decided to investigate the relative energy and structure of a salt formed by combining the $[(MgF_3)_2]^{2-}$ dianion with two counterions, and we selected $Na_2[(MgF_3)_2]$ as a candidate salt. According to our predictions, $[(MgF_3)_2]^{2-}$ is expected to form a geometrically stable $Na_2[(MgF_3)_2]$ molecule when combined with two sodium cations. The equilibrium structure of $Na_2[(MgF_3)_2]$ depicted in Fig. 6 resembles that of the isolated $[(MgF_3)_2]^{2-}$ dianion (see Fig. 1) accompanied by two $Na^+$ cations localized at its two termini. This structure makes sense as it minimizes the Coulomb repulsion between the two cations while maximizing the Coulomb attractions between the cations and the dianion. Comparing the bond lengths and valence angles in the $(MgF_3)_2$ fragments for $[(MgF_3)_2]^{2-}$ and $Na_2[(MgF_3)_2]$ reveals that the Mg-F distances change only slightly (by less than 0.05 Å) upon the formation of $Na_2[(MgF_3)_2]$ whereas the valence angles either remain nearly the same (for the central rhombic $(MgF)_2$ fragment) or change significantly (for the terminal $F_2Mg$ fragments), see Figs. 1 and 6. Namely, the terminal F-Mg-F angles decrease by ca. 20° when two $Na^+$ cations are attached to $[(MgF_3)_2]^{2-}$ and this results in the elongation of the $[(MgF_3)_2]$ moiety.

In order to verify the thermodynamic stability of $Na_2[(MgF_3)_2]$, we examined the most probable fragmentation reactions that this system might be susceptible to. In particular, we considered the fragmentation paths leading to formation of various species ($NaMgF_3$, $NaMg_2F_5$, $MgF_2$, $NaF$, $Mg_2F_4$, $Na_2$, $F_2$, $[Na(MgF_3)_2]^-$, $[(MgF_3)_2]^{2-}$, and $Na^+$) that likely represent the most stable fragmentation products. Since the energies for all these reactions turned out to be positive (see the $\Delta E_r$ values shown in Table 2), none of them should be considered favorable, which confirms the thermodynamic stability of $Na_2[(MgF_3)_2]$.

The results of the population analysis based on the NBO scheme indicates that the partial atomic charges on the $(MgF_3)_2$ fragment in $Na_2[(MgF_3)_2]$ sum up to $-1.850e$ while each of the Na holds a positive partial atomic charge of $+0.925e$, as shown in Fig. 6. Such a charge

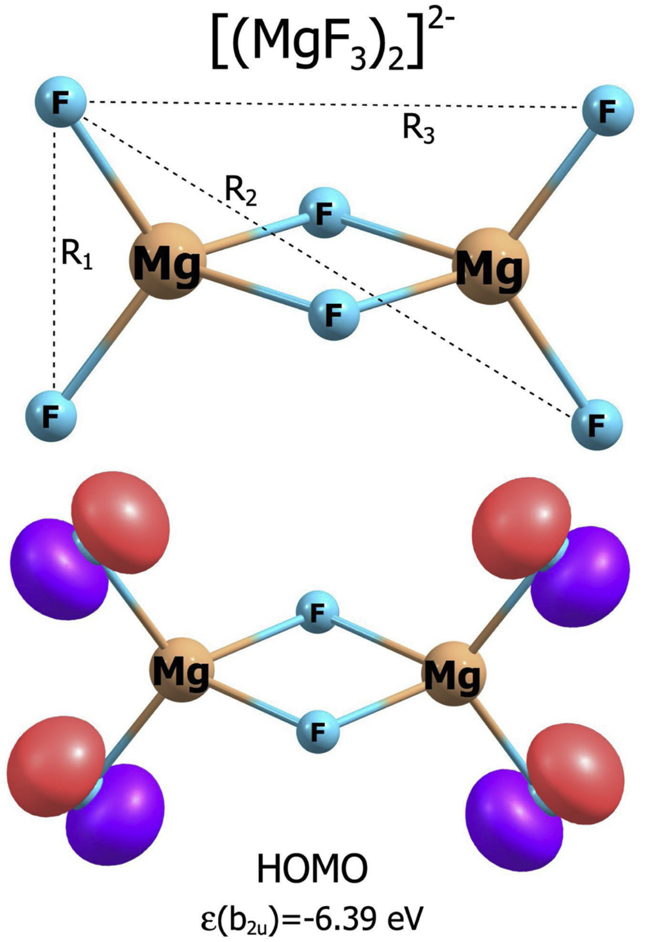

**Fig. 5.** Definition of the separations (R) used in the extended RCB model (top) and the highest occupied molecular orbital (HOMO) for $[(MgF_3)_2]^{2-}$ (bottom).

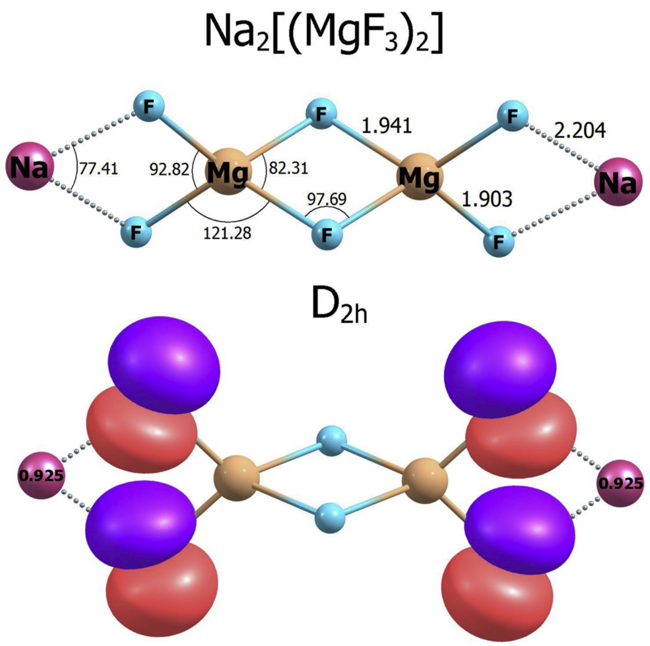

**Fig. 6.** The equilibrium structure of the $Na_2[(MgF_3)_2]$ salt (bond lengths in Å, valence angles in degrees) and the highest occupied molecular orbital of this system. The partial atomic charges on the sodium atoms are provided in a.u.

**Table 2**
The reaction energies[a] ($\Delta E_r$ in kcal/mol) evaluated for various fragmentation processes involving the $Na_2[(MgF_3)_2]$ salt.

| Process | $\Delta E_r$ |
|---|---|
| $Na_2[(MgF_3)_2] \rightarrow 2NaMgF_3$ | 61.2 |
| $Na_2[(MgF_3)_2] \rightarrow NaMg_2F_5 + NaF$ | 66.6 |
| $Na_2[(MgF_3)_2] \rightarrow 2MgF_2 + 2NaF$ | 204.3 |
| $Na_2[(MgF_3)_2] \rightarrow Mg_2F_4 + 2NaF$ | 139.2 |
| $Na_2[(MgF_3)_2] \rightarrow Na_2 + 2MgF_2 + F_2$ | 372.5 |
| $Na_2[(MgF_3)_2] \rightarrow Na_2 + Mg_2F_4 + F_2$ | 307.5 |
| $Na_2[(MgF_3)_2] \rightarrow [Na(MgF_3)_2]^- + Na^+$ | 119.4 |
| $Na_2[(MgF_3)_2] \rightarrow [(MgF_3)_2]^{2-} + 2Na^+$ | 333.6 |

[a] Reported $\Delta E_r$ values include zero-point vibrational energies.

distribution and the fact that the HOMO for $Na_2[(MgF_3)_2]$ is delocalized only among fluorine atoms indicate that the $Na_2[(MgF_3)_2]$ salt is strongly ionic and can be described by the $(Na^+)_2[(MgF_3)_2]^{2-}$ formula.

## 4. Conclusions

On the basis of our quantum chemical calculations performed with the CCSD(T) method and the 6-311+G(d) basis set for $[(MgF_3)_2]^{2-}$ and $[(MgF_3)_2]^-$, whose equilibrium structures and vertical electron binding energies were determined respectively at the MP2/6-311+G(d) and OVGF/6-311+G(3df) levels, we arrive at the following conclusions:

(i) $[(MgF_3)_2]^{2-}$ is a geometrically stable system adopting a $D_{2h}$-symmetry structure with its two excess electrons delocalized evenly among four terminal fluorine atoms.
(ii) $[(MgF_3)_2]^{2-}$ is electronically stable (i.e., it is not expected to spontaneously eject an electron) and its vertical and adiabatic electron binding energies are predicted to be 5.58 and 2.28 eV, respectively.
(iii) Although $[(MgF_3)_2]^{2-}$ is thermodynamically unstable with respect to two fragmentation reactions, neither of these processes would be operative at low internal energies because of large activation barriers that would have to be overcome to render them plausible (i.e., the expected rate of passage over either of these two barriers renders the $[(MgF_3)_2]^{2-}$ dianion kinetically very long-lived).
(iv) Applying the *extended Repulsive Coulomb Barrier model* to $[(MgF_3)_2]^{2-}$ provides an explanation of the difference between its first vertical electron binding energy (5.58 eV) and the vertical electron binding energy of the $[MgF_3]-$ superhalogen anion (8.79 eV).
(v) The $[(MgF_3)_2]^{2-}$ dianion might form thermodynamically stable ionic salts (such as $Na_2[(MgF_3)_2]$) when accompanied by counterions.

Taking into account that $[(MgF_3)_2]^{2-}$ is not expected to spontaneously eject an electron and, despite its metastability, is predicted to be kinetically very long-lived, we conclude that this species is likely to be detected in electrospray mass spectroscopic studies if one could synthesize salts such as $Na_2[(MgF_3)_2]$ to use in the electrospray source solution.

## Acknowledgments

This research was supported by the Polish Ministry of Science and Higher Education [grant No. BMN 538-8370-B736-17/18 (to S.F.)]; and partially by the Polish Ministry of Science and Higher Education [grant No. DS 530-8375-D499-19 (to P.S.)]. The calculations have been carried out using resources provided by Wroclaw Centre for Networking and Supercomputing (http://wcss.pl) [grants No. 436 and 455].

## References

[1] G.L. Gutsev, A.I. Boldyrev, DVM-Xα calculations on the ionization potentials of MX$_{k+1}^{-}$ complex anions and the electron affinities of MX$_{k+1}$ "superhalogens", Chem. Phys. 56 (1981) 277–283, https://doi.org/10.1016/0301-0104(81)80150-4.

[2] S. Freza, P. Skurski, Enormously large (approaching 14 eV!) electron binding energies of [H$_n$F$_{n+1}$]$^-$ (n = 1-5, 7, 9, 12) anions, Chem. Phys. Lett. 487 (2010) 19–23, https://doi.org/10.1016/j.cplett.2010.01.022.

[3] M. Czapla, O. Ciepła, J. Brzeski, P. Skurski, Formation of enormously strongly bound anionic clusters predicted in binary superacids, J. Phys. Chem. A 122 (2018) 8539–8548, https://doi.org/10.1021/acs.jpca.8b07514.

[4] G.L. Gutsev, A.I. Boldyrev, The electronic structure of superhalogens and superalkalies, Russ. Chem. Rev. 56 (1987) 519–531, https://doi.org/10.1070/RC1987v056n06ABEH003287.

[5] S. Giri, S. Behera, P. Jena, Superhalogens as building blocks of halogen-free electrolytes in lithium-ion batteries, Angew. Chem. Int. Ed. 53 (2014) 13916–13919, https://doi.org/10.1002/anie.201408648.

[6] I. Anusiewicz, P. Skurski, Unusual structures of Mg$_2$F$_5^-$ superhalogen anion, Chem. Phys. Lett. 440 (2007) 41–44, https://doi.org/10.1016/j.cplett.2007.04.016.

[7] J. Yang, X. Bin Wang, X.P. Xing, L.S. Wang, Photoelectron spectroscopy of anions at 118.2 nm: observation of high electron binding energies in superhalogens MCl$_4^-$ (M=Sc, Y, La), J. Chem. Phys. 128 (2008), https://doi.org/10.1063/1.2938390 201102.

[8] B. Yin, J. Li, H. Bai, Z. Wen, Z. Jiang, Y. Huang, The magnetic coupling in manganese-based dinuclear superhalogens and their analogues. A theoretical characterization from a combined DFT and BS study, Phys. Chem. Chem. Phys. 14 (2012) 1121–1130, https://doi.org/10.1039/c1cp22928a.

[9] Y. Yu, C. Li, B. Yin, J.L. Li, Y.H. Huang, Z.Y. Wen, Z.Y. Jiang, Are trinuclear superhalogens promising candidates for building blocks of novel magnetic materials? A theoretical prospect from combined broken-symmetry density functional theory and ab initio study, J. Chem. Phys. 139 (2013) 054305, , https://doi.org/10.1063/1.4817189.

[10] L.P. Ding, X.Y. Kuang, P. Shao, M.M. Zhong, Y.R. Zhao, Formation and properties of iron-based magnetic superhalogens: a theoretical study, J. Chem. Phys. 139 (2013) 104304, , https://doi.org/10.1063/1.4819912.

[11] Y.Y. Sun, J.F. Li, M.M. Li, F.Q. Zhou, J.L. Li, B. Yin, Could the description on polynuclear superhalogens by DFT be comparable with high-level ab initio results? A comparison between DFT and CCSD(T), J. Chem. Phys. 144 (2016) 054303, , https://doi.org/10.1063/1.4941056.

[12] C. Sikorska, Are noble gas molecules able to exhibit a superhalogen nature? RSC Adv. 6 (2016) 103418–103427, https://doi.org/10.1039/c6ra21933k.

[13] P. Jena, Superhalogens: a bridge between complex metal hydrides and Li ion batteries, J. Phys. Chem. Lett. 6 (2015) 1119–1125, https://doi.org/10.1021/acs.jpclett.5b00006.

[14] G.L. Gutsev, R.J. Bartlett, A.I. Boldyrev, J. Simons, Adiabatic electron affinities of small superhalogens: LiF$_2$, LiCl$_2$, NaF$_2$, and NaCl$_2$, J. Chem. Phys. 107 (1997) 3867–3875, https://doi.org/10.1063/1.474764.

[15] G.L. Gutsev, P. Jena, R.J. Bartlett, Structure and stability of BF$_3$*F and AlF$_3$*F superhalogens, Chem. Phys. Lett. 292 (1998) 289–294, https://doi.org/10.1016/S0009-2614(98)00716-7.

[16] I. Anusiewicz, P. Skurski, An ab initio study on BeX$_3^-$ superhalogen anions (X = F, Cl, Br), Chem. Phys. Lett. 358 (2002) 426–434, https://doi.org/10.1016/S0009-2614(02)00666-8.

[17] A.N. Alexandrova, A.I. Boldyrev, Y.J. Fu, X. Yang, X. Bin Wang, L.S. Wang, Structure of the Na$_x$Cl$_{x+1}$ (x=1-4) clusters via ab initio genetic algorithm and photoelectron spectroscopy, J. Chem. Phys. 121 (2004) 5709–5719, https://doi.org/10.1063/1.1783276.

[18] B.M. Elliott, E. Koyle, A.I. Boldyrev, X. Bin Wang, L.S. Wang, MX$_3^-$superhalogens (M = Be, Mg, Ca; X = Cl, Br): a photoelectron spectroscopic and ab initio theoretical study, J. Phys. Chem. A 109 (2005) 11560–11567, https://doi.org/10.1021/jp054036v.

[19] H.J. Zhai, L.M. Wang, S.D. Li, L.S. Wang, Vibrationally resolved photoelectron spectroscopy of BO$^-$ and BO$_2^-$: a joint experimental and theoretical study, J. Phys. Chem. A 111 (2007) 1030–1035, https://doi.org/10.1021/jp0666939.

[20] X. Bin Wang, C.F. Ding, L.S. Wang, A.I. Boldyrev, J. Simons, First experimental photoelectron spectra of superhalogens and their theoretical interpretations, J. Chem. Phys. 110 (1999) 4763–4771, https://doi.org/10.1063/1.478386.

[21] S. Smuczyńska, P. Skurski, Is hydrogen capable of playing a central atom role in superhalogen anions? Chem. Phys. Lett. 443 (2007) 190–193, https://doi.org/10.1016/j.cplett.2007.06.075.

[22] M. Marchaj, S. Freza, P. Skurski, Why are SiX$_5^-$ and GeX$_5^-$ (X = F, Cl) stable but not CF$_5^-$and CCl$_5$-? J. Phys. Chem. A 116 (2012) 1966–1973, https://doi.org/10.1021/jp300251t.

[23] S. Smuczyńska, P. Skurski, Halogenoids as ligands in superhalogen anions, Inorg. Chem. 48 (2009) 10231–10238, https://doi.org/10.1021/ic901253r.

[24] I. Anusiewicz, Electrophilic substituents as ligands in superhalogen anions, J. Phys. Chem. A 113 (2009) 6511–6516, https://doi.org/10.1021/jp901910q.

[25] I. Anusiewicz, Superhalogen anions utilizing acidic functional groups as ligands, J. Phys. Chem. A 113 (2009) 11429–11434, https://doi.org/10.1021/jp907246w.

[26] J.F. Li, M.M. Li, H. Bai, Y.Y. Sun, J.L. Li, B. Yin, Probing the properties of polynuclear superhalogens without halogen ligand via ab initio calculations: a case study on double-bridged [Mg$_2$(CN)$_5$]$^{-1}$ anions, ChemPhysChem. 16 (2015) 3652–3659, https://doi.org/10.1002/cphc.201500517.

[27] J.F. Li, Y.Y. Sun, H. Bai, M.M. Li, J.L. Li, B. Yin, Are superhalogens without halogen ligand capable of transcending traditional halogen-based superhalogens? Ab initio case study of binuclear anions based on pseudohalogen ligand, AIP Adv. 5 (2015) 067143, , https://doi.org/10.1063/1.4922958.

[28] B. Yin, T. Li, J.-F. Li, Y. Yu, J.-L. Li, Z.-Y. Wen, Z.-Y. Jiang, Are polynuclear superhalogens without halogen atoms probable? A high-level *ab initio* case study on triple-bridged binuclear anions with cyanide ligands, J. Chem. Phys. 140 (2014) 094301, , https://doi.org/10.1063/1.4867009.

[29] R.-F. Zhao, L. Yu, F.-Q. Zhou, J.-F. Li, B. Yin, Could the increased structural versatility imposed by non-halogen ligands bring something new for polynuclear superhalogens? A case study on binuclear [Mg$_2$L$_5$]$^-$ (L = –OH, –OOH and –OF) anions, Phys. Chem. Chem. Phys. 19 (2017) 26986–26995, https://doi.org/10.1039/C7CP05037B.

[30] M. Willis, M. Götz, A.K. Kandalam, G.F. Ganteför, P. Jena, Hyperhalogens: discovery of a new class of highly electronegative species, Angew. Chem. Int. Ed. 49 (2010) 8966–8970, https://doi.org/10.1002/anie.201002212.

[31] C. Paduani, M.M. Wu, M. Willis, P. Jena, Theoretical study of the stability and electronic structure of Al(BH$_4$)$_{n=1\to4}$ and Al(BF$_4$)$_{n=1\to4}$ and their hyperhalogen behavior, J. Phys. Chem. A 115 (2011) 10237–10243, https://doi.org/10.1021/jp206330d.

[32] Y. Li, S. Zhang, Q. Wang, P. Jena, Structure and properties of Mn4Cl9: an antiferromagnetic binary hyperhalogen, J. Chem. Phys. 138 (2013) 054309, , https://doi.org/10.1063/1.4776217.

[33] C. Paduani, P. Jena, A recipe for designing molecules with ever-increasing electron affinities, J. Phys. Chem. A 116 (2012) 1469–1474, https://doi.org/10.1021/jp211736e.

[34] J. Simons, P. Skurski, R. Barrios, Repulsive coulomb barriers in compact stable and metastable multiply charged anions, J. Am. Chem. Soc. 122 (2000) 11893–11899, https://doi.org/10.1021/ja001936a.

[35] J. Simons, P. Skurski, The roles of electrostatics in forming molecular anions and dianions, Theor. Prospect Negat. Ions, (2002), pp. 117–138.

[36] X.B. Wang, L.S. Wang, Observation of negative electron-binding energy in a molecule, Nature. 400 (1999) 245–248, https://doi.org/10.1038/22286.

[37] L.S. Wang, X. Bin Wang, Probing free multiply charged anions using photodetachment photoelectron spectroscopy, J. Phys. Chem. A 104 (2000) 1978–1990, https://doi.org/10.1021/jp9940093.

[38] C. Møller, M.S. Plesset, Note on an approximation treatment for many-electron systems, Phys. Rev. 46 (1934) 618–622, https://doi.org/10.1103/PhysRev.46.618.

[39] M. Head-Gordon, J.A. Pople, M.J. Frisch, MP2 energy evaluation by direct methods, Chem. Phys. Lett. 153 (1988) 503–506, https://doi.org/10.1016/0009-2614(88)85250-3.

[40] M.J. Frisch, M. Head-Gordon, J.A. Pople, A direct MP2 gradient method, Chem. Phys. Lett. 166 (1990) 275–280, https://doi.org/10.1016/0009-2614(90)80029-D.

[41] R. Krishnan, J.S. Binkley, R. Seeger, J.A. Pople, Self-consistent molecular orbital methods. XX. A basis set for correlated wave functions, J. Chem. Phys. 72 (1980) 650–654, https://doi.org/10.1063/1.438955.

[42] A.D. McLean, G.S. Chandler, Contracted Gaussian basis sets for molecular calculations. I. Second row atoms, Z=11-18, J. Chem. Phys. 72 (1980) 5639–5648, https://doi.org/10.1063/1.438980.

[43] J. Čížek, On the use of the cluster expansion and the technique of diagrams in calculations of correlation effects in atoms and molecules, Adv. Chem. Phys. 14 (1969) 35–89, https://doi.org/10.1002/9780470143599 ch2..

[44] G.D. Purvis, R.J. Bartlett, A full coupled-cluster singles and doubles model: the inclusion of disconnected triples, J. Chem. Phys. 76 (1982) 1910–1918, https://doi.org/10.1063/1.443164.

[45] R.J. Bartlett, G.D. Purvis, Many-body perturbation theory, coupled-pair many-electron theory, and the importance of quadruple excitations for the correlation problem, Int. J. Quantum Chem. 14 (1978) 561–581, https://doi.org/10.1002/qua.560140504.

[46] G.E. Scuseria, C.L. Janssen, H.F. Schaefer, An efficient reformulation of the closed-shell coupled cluster single and double excitation (CCSD) equations, J. Chem. Phys. 89 (1988) 7382–7387, https://doi.org/10.1063/1.455269.

[47] K. Fukui, The path of chemical reactions – the IRC approach, Acc. Chem. Res. 14 (1981) 363–368, https://doi.org/10.1021/ar00072a001.

[48] H.P. Hratchian, H.B. Schlegel, Accurate reaction paths using a Hessian based predictor-corrector integrator, J. Chem. Phys. 120 (2004) 9918–9924, https://doi.org/10.1063/1.1724823.

[49] H.P. Hratchian, H.B. Schlegel, Using Hessian updating to increase the efficiency of a Hessian based predictor-corrector reaction path following method, J. Chem. Theory Comput. 1 (2005) 61–69, https://doi.org/10.1021/ct0499783.

[50] H.P. Hratchian, H.B. Schlegel, Finding minima, transition states, and following reaction pathways on ab initio potential energy surfaces, Theory Appl. Comput. Chem, (2005), pp. 195–249, https://doi.org/10.1016/B978-044451719-7/50053-6.

[51] V.G. Zakrzewski, J.V. Ortiz, J.A. Nichols, D. Heryadi, D.L. Yeager, J.T. Golab, Comparison of perturbative and multiconfigurational electron propagator methods, Int. J. Quantum Chem. 60 (1996) 29–36 doi:10.1002/(SICI)1097-461X(1996)60:1 < 29::AID-QUA3 > 3.0.CO;2-7.

[52] J. Simons, Direct calculation of first- and second-order density matrices, The higher RPA method, J. Chem. Phys. 55 (1971) 1218–1230, https://doi.org/10.1063/1.1676208.

[53] J.V. Ortiz, Electron binding energies of anionic alkali metal atoms from partial fourth order electron propagator theory calculations, J. Chem. Phys. 89 (1988) 6348–6352, https://doi.org/10.1063/1.455401.

[54] D.J. Rowe, Equations-of-motion method and the extended shell model, Rev. Mod. Phys. 40 (1968) 153–166, https://doi.org/10.1103/RevModPhys.40.153.

[55] L.S. Cederbaum, One-body Green's function for atoms and molecules: theory and application, J. Phys. B At. Mol. Opt. Phys. 8 (1975) 290–303, https://doi.org/10.

1088/0022-3700/8/2/018.

[56] J. Simons, Energy-shift theory of low-lying excited electronic states of molecules, J. Chem. Phys. 57 (1972) 3787–3792, https://doi.org/10.1063/1.1678845.

[57] J. Simons, W.D. Smith, Theory of electron affinities of small molecules, J. Chem. Phys. 58 (1973) 4899–4907, https://doi.org/10.1063/1.1679074.

[58] V.G. Zakrzewski, J.V. Ortiz, Semidirect algorithms for third-order electron propagator calculations, Int. J. Quantum Chem. 53 (1995) 583–590, https://doi.org/10.1002/qua.560530602.

[59] V.G. Zakrzewski, J.V. Ortiz, Semidirect algorithms in electron propagator calculations, Int. J. Quantum Chem. 52 (1994) 23–27, https://doi.org/10.1002/qua.560520806.

[60] V.G. Zakrzewski, O. Dolgounitcheva, J.V. Ortiz, Electron binding energies of TCNQ and TONE, J. Chem. Phys. 105 (1996) 5872–5877, https://doi.org/10.1063/1.472428.

[61] K. Pradhan, G.L. Gutsev, P. Jena, Negative ions of transition metal-halogen clusters, J. Chem. Phys. 133 (2010) 144301, , https://doi.org/10.1063/1.3489117.

[62] J.P. Foster, F. Weinhold, Natural hybrid orbitals, J. Am. Chem. Soc. 102 (1980) 7211–7218, https://doi.org/10.1021/ja00544a007.

[63] A.E. Reed, F. Weinhold, Natural bond orbital analysis of near-Hartree-Fock water dimer, J. Chem. Phys. 78 (1983) 4066–4073, https://doi.org/10.1063/1.445134.

[64] A.E. Reed, R.B. Weinstock, F. Weinhold, Natural population analysis, J. Chem. Phys. 83 (1985) 735–746, https://doi.org/10.1063/1.449486.

[65] J.E. Carpenter, F. Weinhold, Analysis of the geometry of the hydroxymethyl radical by the "different hybrids for different spins" natural bond orbital procedure, J. Mol. Struct. THEOCHEM. 169 (1988) 41–62, https://doi.org/10.1016/0166-1280(88)80248-3.

[66] A.E. Reed, L.A. Curtiss, F. Weinhold, Intermolecular interactions from a natural bond orbital, donor-acceptor viewpoint, Chem. Rev. 88 (1988) 899–926, https://doi.org/10.1021/cr00088a005.

[67] M.J. Frisch, G.W. Trucks, H.B. Schlegel, G.E. Scuseria, M.A. Robb, J.R. Cheeseman, G. Scalmani, V. Barone, G.A. Petersson, H. Nakatsuji, X. Li, M. Caricato, A.V. Marenich, J. Bloino, B.G. Janesko, R. Gomperts, B. Mennucci, H.P. Hratchian, J.V. Ortiz, A.F. Izmaylov, J.L. Sonnenberg, D. Williams-Young, F. Ding, F. Lipparini, F. Egidi, J. Goings, B. Peng, A. Petrone, T. Henderson, D. Ranasinghe, V.G. Zakrzewski, J. Gao, N. Rega, G. Zheng, W. Liang, M. Hada, M. Ehara, K. Toyota, R. Fukuda, J. Hasegawa, M. Ishida, T. Nakajima, Y. Honda, O. Kitao, H. Nakai, T. Vreven, K. Throssell, J. Montgomery, J. A, F. Peralta, J.E. Ogliaro, J.J. Bearpark, M.J. Heyd, K.N. Brothers, E.N. Kudin, V.N. Staroverov, T.A. Keith, R. Kobayashi, J. Normand, K. Raghavachari, A.P. Rendell, J.C. Burant, S.S. Iyengar, J. Tomasi, M. Cossi, J.M. Millam, M. Klene, C. Adamo, R. Cammi, J.W. Ochterski, R.L. Martin, K. Morokuma, O. Farkas, J.B. Foresman, D.J. Fox, Gaussian 16,Revision B.01, Wallingford CT, (2016).

[68] I. Anusiewicz, M. Sobczyk, I. Dąbkowska, P. Skurski, An ab initio study on $MgX_3^-$ and $CaX_3$- superhalogen anions (X = F, Cl, Br), Chem. Phys. 291 (2003) 171–180, https://doi.org/10.1016/S0301-0104(03)00208-8.